EurJIC European Journal of Inorganic Chemistry

ChemPubSoc Europe

FULL PAPER

DOI:10.1002/ejic.201300366

An Electrochemical and Raman Spectroscopy Study of the Surface Behaviour of Mononuclear Ruthenium and Osmium Polypyridyl Complexes Based on Pyridyl- and Thiophene-Based Linkers

Yvonne Halpin,[a] Hella Logtenberg,[b] Laura Cleary,[a] Stephan Schenk,[c] Martin Schulz,[d] Apparao Draksharapu,[b] Wesley R. Browne,*[b] and Johannes G. Vos*[a]

Keywords: Ruthenium / Osmium / Self-assembled monolayer / Raman spectroscopy / Electrochemistry

The utility of a thiophene anchor unit as an alternative for thiols in the immobilisation of ruthenium and osmium complexes on gold and platinum is examined with special attention focused on the relative contributions of physi- and chemisorption of the complexes and the chemical stability of the thiophene anchoring unit. The redox and spectroscopic properties of the ruthenium(II) and osmium(II) complexes are described in solution and the effect of surface immobilisation examined through a combined electrochemical and surface-enhanced Raman spectroscopic study. A key finding is that although the thiophene unit is involved in surface anchoring it also undergoes chemical reactions with the gold surface as demonstrated by Raman spectroscopy.

Introduction

The bottom-up approach[1,2] to the construction of molecular-based electronic devices through self-assembly has been at the forefront of efforts[3] to apply organic and molecular inorganic components as molecular junctions,[4] wires,[1–3,5] transistors[6] and diodes.[7] These efforts face many limitations absent in solid-state devices and as a result many of the molecular-based devices reported in the literature have been studied under cryogenic and/or ultra-high vacuum conditions.[6b,6c] Hence, a major hurdle in the implementation of molecular systems in electronic devices is to achieve operation at ambient conditions. Monolayers based on osmium complexes modified with 4,4′-bipyridyl-based linkers have been investigated since the mid-1990s (Figure 1),[8] and have been shown to display transistor-like behaviour at room temperature in aqueous solution when assembled on platinum and gold surfaces.[9] The nature of the linker, such as a pyridine or thiol group[10] (see Figure 1), is an important structural component since it is expected to control, to a large extent, interfacial electron-transfer properties between the redox centre and the electrode surface.[11] Overall, most focus has been placed on aryl and alkyl thiol anchoring units, however, although convenient for the formation of self-assembled monolayers, SAMs, the synthesis of the precursors is generally challenging and has limited to some extent the availability of variation in the molecular systems studied. The development of other linkers for surface attachment is, therefore, of continuing interest and alternative options include pyridine and thiophene. In the latter case, relatively little is known about its interaction with gold surfaces.[12]

In this contribution, we report the electrochemical and spectroscopic properties of a series of Ru^{II} and Os^{II} polypyridyl complexes of the general formula $[M(bpy)_2L]^{2+}$ where M is either Ru^{II} or Os^{II}, bpy is 2,2′-bipyridyl and L represents either the ligand 2-(4-pyridyl)imidazole[*f*]-1,10-phenanthroline (pyrphen) or 2-(3-thiophenyl)imidazole[*f*]-1,10-phenanthroline (thimphen) (see Figure 2) both in solution and as monolayers on Pt and Au. The complexes are structurally similar, differing only in the linker unit they contain; pyridine vs. thiophene. The aim of these studies is to investigate the potential of these moieties as anchors for the immobilisation of metal complexes. The synthesis, electrochemical and spectroscopic properties of the compounds in solution are reported together with the investigation of self-assembled monolayers of the complexes, which are

[a] Solar Energy Conversion SRC, School of Chemical Sciences, Dublin City University,
Dublin 9, Ireland
Fax: +353-1-7005503
E-mail: han.vos@dcu.ie
[b] Stratingh Institute for Chemistry and Zernike Institute for Advanced Materials, Faculty of Mathematics and Natural Sciences, University of Groningen,
Nijenborgh 4, 9747 AG Groningen, The Netherlands
E-mail: w.r.browne@rug.nl
Homepage: www.rug.nl/stratingh, w.r.browne@rug.nl
[c] BASF SE, Material Physics and Analytics,
Carl-Bosch-Str. 38, 67056 Ludwigshafen, Germany
[d] Pharmaceutical Radiochemistry, Technical University, Munich,
Walther-Meißner-Str. 3, 85748 Garching, Germany
Supporting information for this article is available on the WWW under http://dx.doi.org/10.1002/ejic.201300366.

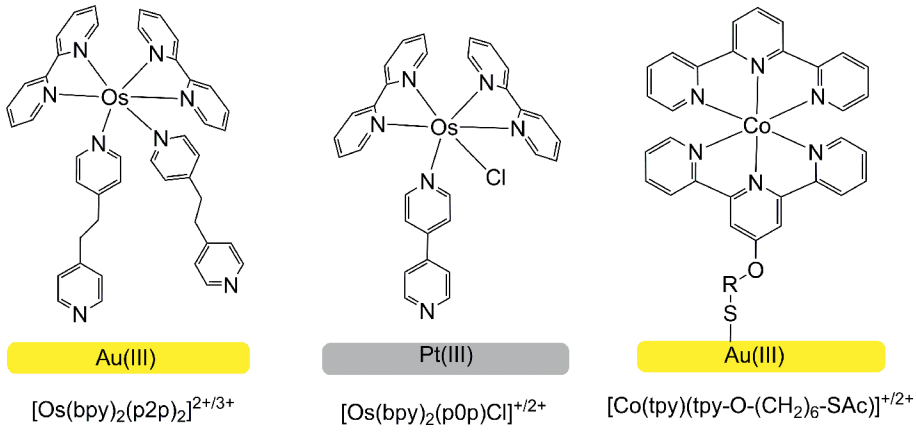

Figure 1. Molecular structures of the Os and Co complexes bound to Pt and Au surfaces where bpy = 2,2′-bipyridine, p0p = 4,4′-bipyridine, p2p = 1,2-bis(4′-pyridyl)ethane, tpy = 2,2′,2′′-terpyridine and Ac = acetyl.

characterised by electrochemical techniques and surface-enhanced Raman scattering (SERS) spectroscopy.

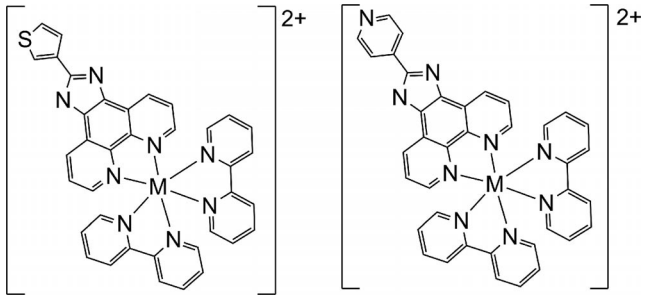

Figure 2. Structures of $[M(bpy)_2(thimphen)]^{2+}$ and $[M(bpy)_2(pyrphen)]^{2+}$, where M = Ru^{II} or Os^{II}, respectively.

Results and Discussion

Synthesis

The ligand thimphen was synthesised in moderate yield using a modified literature procedure[13] (see Supporting Information). The complexes $[Ru(bpy)_2(thimphen)]^{2+}$ and $[Os(bpy)_2(thimphen)]^{2+}$ were obtained in good yield by the treatment of thimphen with $[M(bpy)_2Cl_2]\cdot 2H_2O$, where M = Ru or Os. However, the synthesis of pyrphen was problematic and an alternative preparation method was used, where the $[M(bpy)_2(1,10\text{-phenanthroline})]^{2+}$ precursor was oxidised to the corresponding 1,2-diketone followed by the formation of the pyridine imidazole unit (Figure 3).

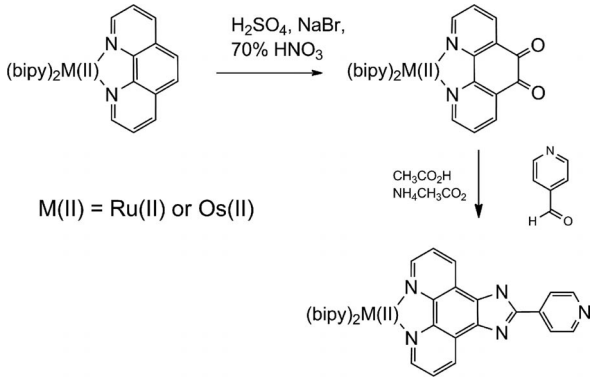

Figure 3. Reaction scheme for the "on complex" synthesis of the metal complex $[Ru(bpy)_2(pyrphen)]^{2+}$.

The ^1H NMR spectra (see Supporting Information) of the ligands are as expected.[13] The spectra of the metal complexes were assigned by comparison with spectra of isotopologues of the complexes (Figures S1–3). Electrospray ionisation mass spectrometry (ESI-MS) shows base signals for the thimphen-based complexes corresponding to $[M - 2(PF_6) - 1]^+$ rather than the expected $[M - 2(PF_6)]^{2+}$ ions, indicating that the imidazole ligand deprotonates upon ionisation. The pyrphen-based complexes show $[M - PF_6]^+$ and $[M - 2PF_6]^{2+}$ as the base signals.

UV/Vis Absorption and Emission Spectroscopy and Acid/Base Chemistry

UV/Vis absorption and emission data are provided in Table 1. The UV/Vis absorption spectra are dominated by strong absorptions in the visible region, assigned as metal-to-ligand charge-transfer (^{1}MLCT) transitions.[14] The osmium complexes also display less intense absorptions at ca. 600 nm, which are assigned to, formally, forbidden ^{3}MLCT transitions.[15] All four complexes show the expected ^{3}MLCT emission at room temperature in acetonitrile.[14,16] Notably in each case a slight redshift in emission is observed on going from the thiophene unit to the pyridine unit indicating, at least modest, electronic communication between the complexes and the peripheral "anchor" groups in the excited state (see Figure 4).

Where ligand moieties that undergo the deprotonation are bound directly to the metal centre, considerable pH-dependent changes in the electronic properties can be expected.[17] However, for the present complexes the changes in the visible part of the absorption spectra are minor with substantial changes confined to the UV region of the spectrum. This suggests that the electronic coupling of the imid-

Table 1. UV/Vis absorption and emission spectroscopic data.[a]

Complex	Absorption λ_{max} [nm] (log ε) [$M^{-1}cm^{-1}$]	Emission λ_{max} [nm]
Ru(thimphen)	424 (3.78)	607
Ru(pyrphen)	435 (3.71)	618
$[Ru(bpy)_2]^{3+}$	450 (4.06)	615[b]
Os(thimphen)	440 (3.85); 600 sh	726
Os(pyrphen)	469 (3.82); 600 sh	748
$[Os(bpy)_2]^{3+}$	468 (4.04); 600 sh[b]	732[c]

[a] In acetonitrile at 298 K. [b] Ref.[33] [c] Ref.[34]

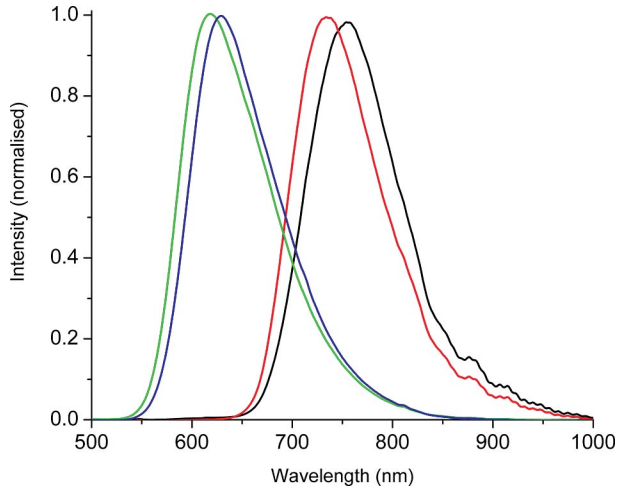

Figure 4. Normalised emission spectra of (from left to right) $[Ru(bpy)_2(thimphen)]^{2+}$, $[Ru(bpy)_2(pyrphen)]^{2+}$, $[Os(bpy)_2(thimphen)]^{2+}$ and $[Os(bpy)_2(pyrphen)]^{2+}$in acetonitrile at 293 K.

azole moiety with the metal centre is limited. The effect of deprotonation of the imidazole moiety[18] on the UV/Vis absorption spectrum of the complexes was examined through a pH titration in aqueous solution (see Supporting Information, Figures S4–S7). For the thimphen-based complexes a pK_a of 9.0 ± 0.1 was determined for the deprotonation of the imidazole moiety. Somewhat surprisingly for the pyridine complex evidence for deprotonation was not observed. These observations are consistent with ESI-MS data (vide supra). In addition to deprotonation, protonation of the imidazole groups may be expected as well and the pH titration monitored by UV/Vis absorption spectroscopy indicated a pK_a of 3.1 ± 0.1 for all complexes. For the pyrphen complexes, no additional changes corresponding to protonation of the pyridine ring were observed.

Resonance Raman Spectroscopy

Resonance Raman spectroscopy can provide useful information for assigning electronic transitions because of the selective enhancement of scattering from vibrational modes associated with the electronic transition resonant with the excitation wavelength used to obtain the Raman spectrum.[19]

The Raman spectrum of each complex was compared with that of $[Ru(bpy)_3]^{2+}$. The Raman (at λ_{exc} = 785 nm) and resonance Raman spectra recorded at λ_{exc} = 355, 449 and 473 nm are shown in Figure 5 and Figure S8. The spectra allow for the assignment of the involvement of the various ligand components in the electronic transitions observed in the visible region of the absorption spectrum. At λ_{exc} = 355 nm, the Raman spectrum is dominated by bands associated with the thimphen and pyrphen ligands consistent with assignment of the absorption at that wavelength to π–π* transitions centred on those ligands. The resonance Raman spectra at λ_{exc} = 449 nm and more so at λ_{exc} = 473 nm contain primarily contributions from the thimphen and pyrphen ligands as well as bpy ligands consistent with the assignment of the visible absorption bands arising from ^{1}MLCT transitions to both the bpy and thim/pyrphen ligands. Importantly, with regard to the discussion on the SERS data of sub-monolayers on gold beads below, the SERS spectrum recorded by aggregation of gold colloid, although similar, shows small differences in peak positions compared with the resonance Raman spectra and the solid-state spectrum.

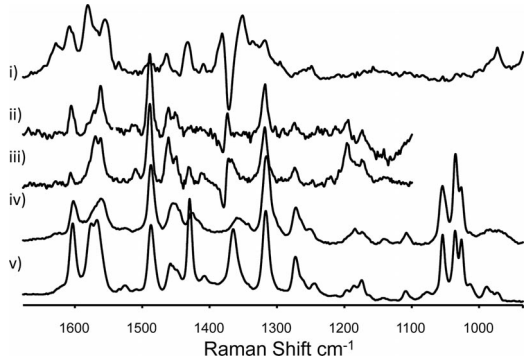

Figure 5. Raman spectra of $[Ru(bpy)_2(thimphen)]^{2+}$, (i) at λ_{exc} = 355 nm, (ii) at λ_{exc} = 449 nm and (iii) at λ_{exc} = 473 nm, 0.1 M in CH_3CN, solvent subtracted and baseline corrected; and (iv) SERS spectrum (Au colloid aggregation) and (v) solid-state spectrum at λ_{exc} = 785 nm.

Computational Results

The frontier orbital region of the ascribed complexes was studied by density functional theory (DFT) calculations. Percent contributions of selected parts of the molecule to the frontier orbitals were calculated by a population analysis and analysed with the GaussSum program. A summary is given in the Supporting Information (Tables S1–S10). The computational investigations included $[M^{II}(bpy)_2(pyrphen)]^{2+}$, $[M^{II}(bpy)_2(thimphen)]^{2+}$, $[M^{III}(bpy)_2(pyrphen)]^{3+}$ and $[M^{III}(bpy)_2(thimphen)]^{3+}$, where M is Ru or Os, as well as the deprotonated complexes $[Ru^{II}(bpy)_2(pyrphen)]^{+}$ and $[Ru^{II}(bpy)_2(thimphen)]^{+}$. As expected the three highest energy occupied molecular orbitals (HOMO, HOMO–1 and HOMO–2) of the $[M^{II}(bpy)_2(pyrphen)]^{2+}$ {see Figure 6 for the HOMO of $[Ru(bpy)_2(pyrphen)]^{2+}$} and $[M^{II}(bpy)_2(thimphen)]^{2+}$ complexes are metal based, which agrees well with the electrochemical data showing metal-based oxidations (vide infra). Both, pyridine and thiophene contribute to HOMO–3 and HOMO–4. The

LUMOs of these complexes are delocalised orbitals with contributions primarily from the bipyridine ligands as well as from the phenanthroline/imidazole moiety but with no contributions from pyridine or thiophene. Higher energy unoccupied orbitals also show contributions from the phenanthroline/imidazole moiety as well as from pyridine. In contrast, thiophene contributions are not found in the first five unoccupied orbitals.

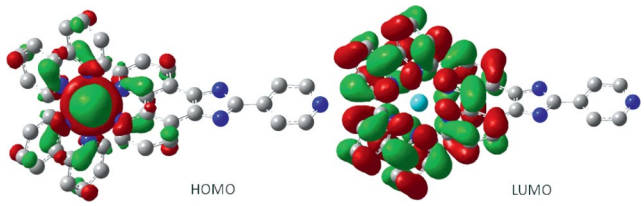

Figure 6. HOMO and LUMO for $[Ru(bpy)_2(pyrphen)]^{2+}$.

Oxidation from the M^{II} to the M^{III} state leads to a rearrangement of the frontier orbitals, with an unpaired electron (α-HOMO). This orbital is delocalised over the phenanthroline/imidazole moiety and pyridine or thiophene of $[Ru^{III}(bpy)_2(pyrphen)]^{3+}$, $[Ru^{III}(bpy)_2(thimphen)]^{3+}$ and $[Os^{III}(bpy)_2(thimphen)]^{3+}$. However, for $[Os^{III}(bpy)_2(pyrphen)]^{3+}$ it is localised just on the pyridine moiety. The involvement of the linker moieties, pyridine and thiophene, in the HOMO is of particular interest. The same arrangement was observed before for the 4,4′-bipyridyl complexes discussed above.[11] Room-temperature scanning tunnelling microscopy, STM, studies showed that for these compounds well-defined electron transfer between the electrode surface, via the redox centre, to an STM tip could be observed establishing the transistor-type behaviour of such molecules.[9] On the basis of the DFT results obtained for the compounds reported in this contribution we postulate that similar electron-transfer processes will be observed, however, since the linkers are different, the electron transfer will take place at different rates for each.

Deprotonation of the imidazole moiety to $[Ru^{II}(bpy)_2(pyrphen)]^{+}$ and $[Ru^{II}(bpy)_2(thimphen)]^{+}$ leads to a phenanthroline/imidazole and pyridine- or thiophene-based HOMO. Three metal-based orbitals are observed at lower energy as HOMO–1 to HOMO–3. The two lowest energy unoccupied orbitals are found to be bipyridine based but no contributions from pyridine or thiophene to the five lowest energy unoccupied orbitals are found. As discussed above, deprotonation of the imidazole moiety is observed for the $[M(bpy)_2(thimphen)]^{2+}$ but not for the $[M(bpy)_2(pyrphen)]^{2+}$ species. The calculations do not yield insight into this unexpected behaviour, but show that upon deprotonation little change is observed in the Ru-based HOMO orbitals but that thimphen-containing orbitals show significant changes in energy. This is in agreement with the pH titrations (vide supra) and confirms that there is little electronic coupling between the metal centre and the imidazole unit in the ground state.

Redox Properties

All four complexes show a single quasi-reversible oxidation at potentials similar to their analogous $[M(bpy)_3]^{2+}$ complexes (where M = Ru or Os) and with no significant difference between the pyridine- and thiophene-based complexes (Table 2) or the analogous Ru^{II} complexes containing the ligands imidazo[4,5-*f*]1,10-phenanthroline (ip) and 2-phenylimidazo[4,5-*f*][1,10]phenanthroline (pip) reported by Zhou et al.[20] In acetonitrile, six reduction processes were observed in the cyclic voltammograms of $[M(bpy)_2(pyrphen)]^{2+}$ (where M = Ru, Os, Figure 7). The LUMO of $[Ru(bpy)_2(pyrphen)]^{2+}$ (Figure 6, Table S1, vide infra) is shown to have 30% contribution from the phen/imidazole unit and a 69% contribution from bipy. This is in agreement with spectroscopic data (vide supra) and the reduction of bpy and phen ligands are largely invariant for a very wide range of complexes (–1.35 V).[3] The potential of the first reduction is observed at –1.24 V (vs. SCE). This reduction is irreversible at slow scan rates, vide infra. An analogous reduction was not observed in the thimphen-based complexes or for the complexes $[Ru(bpy)_2(phen)]^{2+}$ and $[Ru(bpy)_3]^{2+}$ (first reduction at –1.33 and –1.34 V vs. SCE,[21] respectively). The signal at –1.24 V is assigned to a pyridine-based reduction based on the irreversibility and is consistent with the ability of the pyridine unit to undergo proton-coupled reductions.

Further irreversible reduction waves are observed with cathodic peak potentials[23] of –2.07 and –2.64 V. These processes are not fully reversible, and are assigned to the phenanthroline-based ligand.

Table 2. Solution-based electrochemical data.[a]

$[Ru(bpy)_2(pyrphen)]^{2+}$	1.33(60); –1.24(irr); –1.48 (65); –1.73(70); –2.07(70); –2.38(110)*; –2.64(120);
$[Ru(bpy)_2(thimphen)]^{2+}$	1.28(55); –1.37(70); –1.48(80); –1.58(60); –1.98(70); –2.40(150)*; –2.69(120)
$[Ru(bpy)_3]^{2+}$[22]	1.29(70); –1.33(60); –1.52(65); –1.76(65)
$[Ru(bpy)_2(ip)]^{2+}$[20]	1.25; –1.42; –1.66
$[Ru(bpy)_2(pip)]^{2+}$[20]	1.28; –1.41; –1.62
$[Os(bpy)_2(pyrphen)]^{2+}$	0.89(60); –1.18(irr); –1.41(60);–1.70(65); –2.01(80); –2.35(irr)* –2.46(irr)
$[Os(bpy)_2(thimphen)]^{2+}$	0.86(60); –1.27(70); –1.42(80); –1.53(80); –1.92(60); –2.30(irr)*; –2.60(90)
$[Os(bpy)_3]^{2+}$[22]	0.83; –1.28

[a] Vs. SCE in 0.1 M $TBAPF_6$ acetonitrile. Scan rate: 100 mV s^{-1}. GC working electrode (3-mm diameter). *: Electrolyte-based redox process.

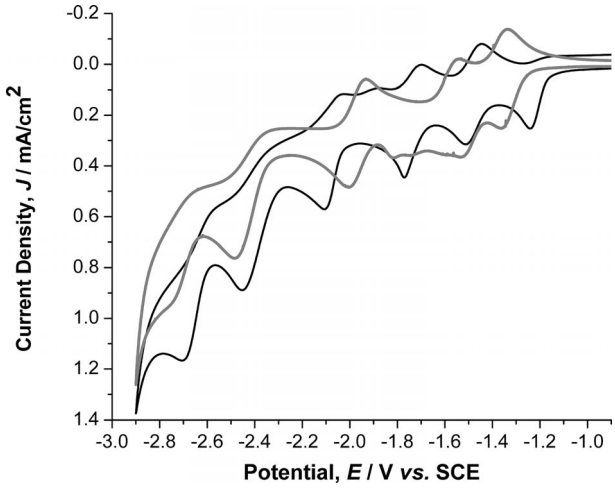

Figure 7. Cyclic voltammetry of $[Ru(bpy)_2(pyrphen)]^{2+}$ (black line) and $[Ru(bpy)_2(thimphen)]^{2+}$ (gray line) at a GC working electrode in CH_3CN (0.1 M $TBAPF_6$) at 100 mV s^{-1}.

Monolayer Formation

Although the thiol anchor group has been employed most widely in the formation of SAMs on gold and, to a lesser extent, platinum surfaces,[10] other anchoring units, such as 4,4′-bipyridine, have also been employed.[8,9] In the present study, SAM formation is expected to be driven by the pyridine and thiophene groups on the complexes (see Figure 2). Of particular interest is the behaviour of thiophene as a potential surface anchoring unit and its stability with regard to chemisorption on gold.

The electrochemical data for SAMs of the four complexes are provided in Table 3 and scan rate-dependent cyclic voltammetry is shown in Figure 8 and Figure 9, as well as Figure S9 (see Supporting Information). The voltammetric peak shapes and potentials do not vary between 1 and 5 V s^{-1}, with current i_p [A] increasing in direct proportion to the scan rate, ν [V s^{-1}], as expected for a surface confined process. The ΔE_p is in between 15 and 25 mV and the full width at half maximum (FWHM) is 100–160 mV, which is slightly larger than the theoretical 90.6 mV for a one-electron process.[24] The surface coverage (Γ) was calculated from the current density at between 2 and 8×10^{-11} mol cm^{-2}, which indicates sub-monolayer coverage. The values of ΔE_p, Γ and FWHM are consistent with related systems, e.g., monolayers of $[Ru(bpy)_2(bpySH)]^{2+}$[25] and $[Ru(bpy)_2(2,2′:4,4′′:4′4′′\text{-quarterpyridyl})]^{2+}$[26] on Pt electrodes.

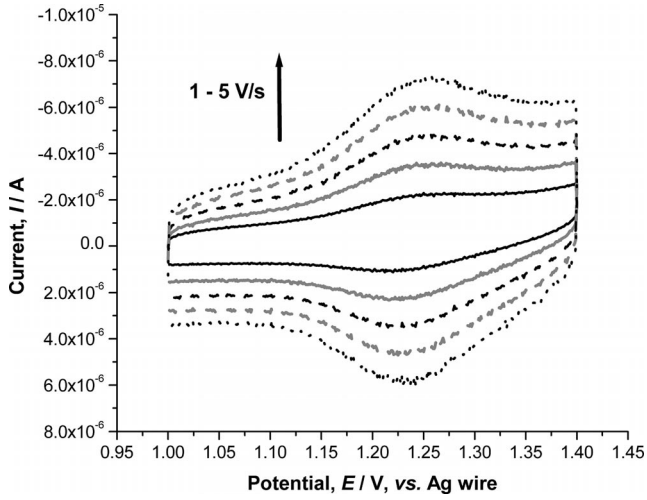

Figure 8. Cyclic voltammetry of $[Ru(bpy)_2(thimphen)]^{2+}$ on a Pt macro electrode (electrochemical surface area: 0.0982 cm^2) vs. SCE, in acetonitrile (0.1 M $TBAClO_4$). The SAM was formed by immersion of the electrode overnight in a 0.5 mM solution of the complex in ethanol followed by rinsing with ethanol and then the electrolyte.

The scan rate dependence of the cyclic voltammetry obtained for $[Os(bpy)_2(thimphen)]^{2+}$ in water shows an additional feature. The first positive sweep segment shows a shift in $E_{p,a}$ by 40 mV to more positive potentials, with the peak potentials returning to the potentials observed in organic solvents on the return and subsequent cycles (Figure 10). Notably this is observed only for the complex $[Os(bpy)_2(thimphen)]^{2+}$ and not the analogous ruthenium complex or either of the pyrphen-based complexes. However, it may be related to the higher surface coverage obtained for $[Os(bpy)_2(thimphen)]^{2+}$. Furthermore the redox potentials of both osmium complexes are ca. 200–250 mV less positive in aqueous solution (with $LiClO_4$) than in acetonitrile (with $TBAClO_4$), Table 3.

Similar effects have been reported by Faulkner and coworkers[8a] for SAMs of the complex $[Os(bpy)_2(p0p)Cl]^+$ (Figure 1), which were rationalised as being because of ion pairing and hence a marked solvent dependence. The observed shift in potential for the initial cycle for an $[Os(bpy)_2(thimphen)]^{2+}$ monolayer in aqueous electrolyte can be assigned tentatively to the uptake of perchlorate ions that are then retained within the monolayer.

Table 3. $E_{½}$ in solution and as SAMs on platinum (Pt) and gold (Au) for all complexes and calculated surface coverage (Γ).[a]

	$E_{½}$ [V] in CH_3CN	$E_{½}$ [V] SAM in CH_3CN	$E_{½}$ [V] SAM in H_2O	Γ[b] [mol cm^{-2}]
$[Ru(bpy)_2(pyrphen)]^{2+}$	+1.31	+1.33 (Pt)	n.a.	2×10^{-11} (CH_3CN)
$[Ru(bpy)_2(thimphen)]^{2+}$	+1.30	+1.24 (Pt)	n.a.	1×10^{-11} (CH_3CN)
$[Os(bpy)_2(pyrphen)]^{2+}$	+0.86	+0.88 (Pt)	+0.67 (Pt)	2.5×10^{-11} (H_2O) 2.5×10^{-11} (CH_3CN)
$[Os(bpy)_2(thimphen)]^{2+}$	+0.83	+0.93 (Au)	+0.68 (Au)	8×10^{-11} (H_2O) 2×10^{-11} (CH_3CN)

[a] Potentials are vs. SCE. In all cases the electrolyte is 0.1 M $LiClO_4$. The electrode used is indicated in parentheses; n.a.: not available. [b] $\pm 0.1 \times 10^{-11}$.

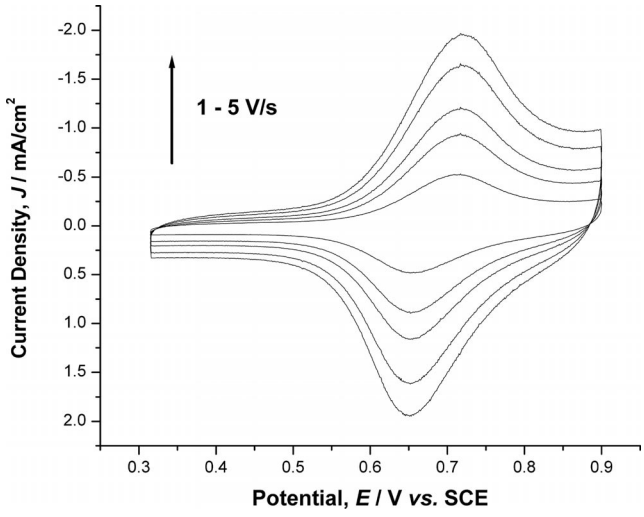

Figure 9. Cyclic voltammetry of $[Os(bpy)_2(thimphen)]^{2+}$ assembled on a Au bead electrode (electrochemical surface area: 0.04 cm^2) following immersion overnight in a 0.5 mM solution in ethanol, followed by rinsing with ethanol and then the electrolyte, vs. SCE, 0.1 M $LiClO_4$ in H_2O.

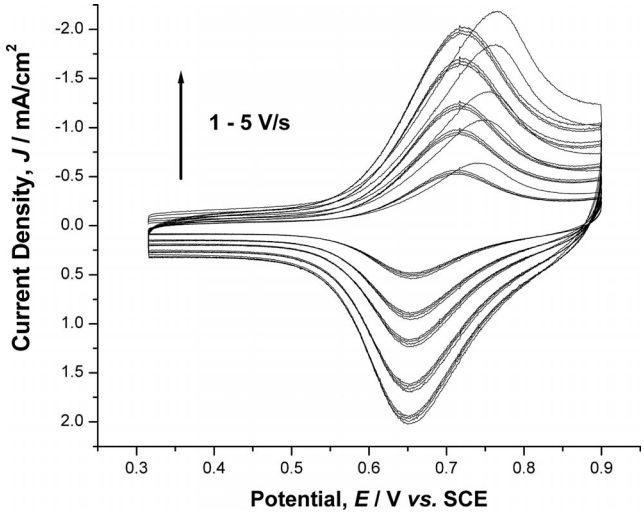

Figure 10. Cyclic voltammetry of a SAM of $[Os(bpy)_2(thimphen)]^{2+}$ [formed on a Au bead electrode (electrochemical surface area: 0.0424 cm^2) by overnight immersion in a 0.5 mM solution in ethanol followed by rinsing with ethanol and then the electrolyte] in 0.1 M $LiClO_4$(aq.) vs. SCE.

Surface-Enhanced Raman Spectroscopy

Surface-enhanced Raman scattering (SERS) spectroscopy, using both gold colloid and electrochemically roughened gold beads, was applied to probe the nature of the interaction between the thiophene bearing complexes and gold. The relative importance of chemisorption with respect to physisorption in forming the (sub)monolayers was assessed using $[Ru(bpy)_2(thimphen)]^{2+}$ and its isotopologue $[Ru(D_8\text{-}bpy)_2(thimphen)]^{2+}$. The SERS spectra of $[Ru(bpy)_2(thimphen)]^{2+}$ obtained both by aggregation of gold colloid and from a submonolayer on an electrochemically roughened gold bead are shown in Figure 11. A difference in intensity for several bands as well as conformational broadening are observed when the spectra of $[Ru(bpy)_2(thimphen)]^{2+}$ on a gold bead and on gold colloid are compared.[27] This is especially the case in the low wavenumber region where the relative intensity of the bands is less in the monolayer, possibly due to binding of the thiophene unit to the gold surface.

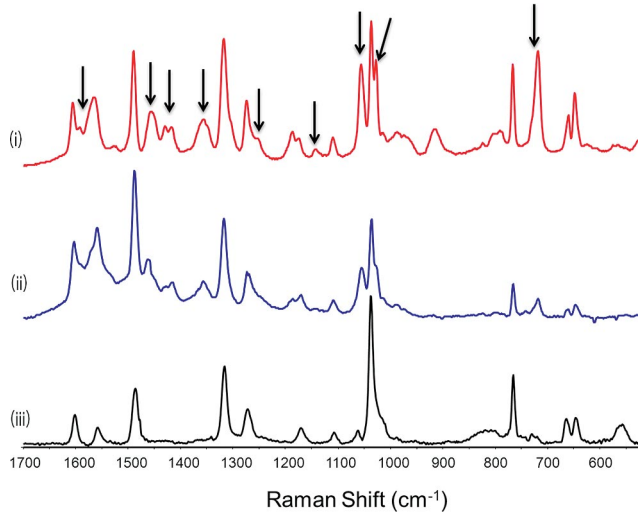

Figure 11. SERS spectra of $[Ru(bpy)_2(thimphen)]^{2+}$ obtained (i) by aggregation of Au colloid, (ii) a SAM formed on an electrochemically roughened Au bead and (iii) the SERS spectrum of $[Ru(bpy)_3]^{2+}$ obtained by aggregation of gold colloid. The arrows indicate thimphen bands. Surfaces were rinsed with ethanol after SAM formation before spectra were recorded.

Assignment of the spectra was made by comparison with the Raman spectra obtained for $[Ru(bpy)_3]^{2+}$ and the isotopologue $[Ru(D_8\text{-}bpy)_2(thimphen)]^{2+}$. The bands arising from the bpy ligands are equal in Raman shift to the spectrum of $[Ru(bpy)_3]^{2+}$. Deuteration of the bipyridine ligands allows for definitive assignment (Figure 12). The SERS spectra of $[Ru(bpy)_2(thimphen)]^{2+}$ and $[Ru(bpy)_2(pyrphen)]^{2+}$ obtained using gold colloid were compared to assign the bands arising from thiophene and phen moieties (Figure 13). The frequencies of each of the vibrational modes of the bpy ligands have been reported at 1608, 1563, 1491, 1320, 1276, 1264, 1176, 1043, 1028, 767 and 668 cm^{-1}.[28] The C–C stretching modes of the bpy ligand give rise to frequencies at 1608, 1563 and 1491 cm^{-1} with the ring modes occurring at 1028, 767 and 668 cm^{-1}. The C–H bend coupled with the ring stretch mode is at 1176 cm^{-1}.[26,28] The bands that are not related to the bpy vibrational modes (see Figure 11) are associated with modes of the pyrphen ligand. The bands at 720 and 1420 cm^{-1} are not observed in the spectrum of $[Ru(bpy)_2(pyrphen)]^{2+}$ and are therefore assigned as thiophene bands.

Importantly, the SERS spectrum of monolayers of $[Ru(bpy)_2(thimphen)]^{2+}$ on gold beads was found to change over time. An increase in intensity and broadening of the band at 650 cm^{-1} together with a decrease in the intensity of the band at 720 cm^{-1} was observed. These data indicate that the thiophene group is affected upon adsorption to a

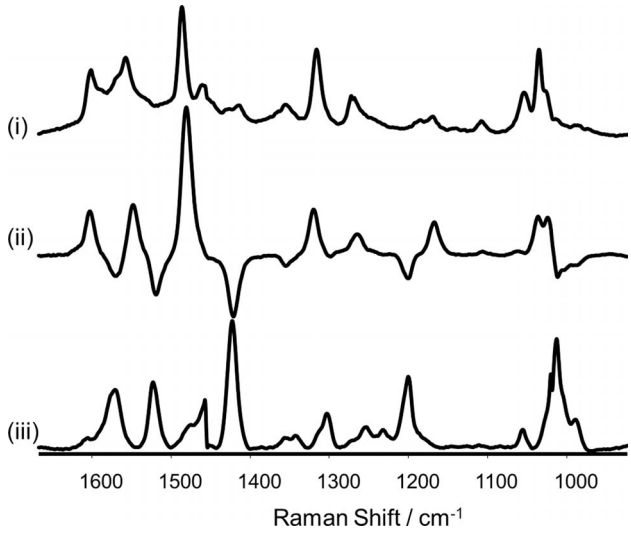

Figure 12. SERS spectra obtained from SAMs of (i) $[Ru(bpy)_2(thimphen)]^{2+}$ and (iii) $[Ru(D_8\text{-}bpy)_2(thimphen)]^{2+}$ on an electrochemically roughened gold bead (λ_{exc} = 785 nm). The difference spectrum (ii) shows the bands associated with $[H_8]$-bpy (positive) and $[D_8]$-bpy (negative).

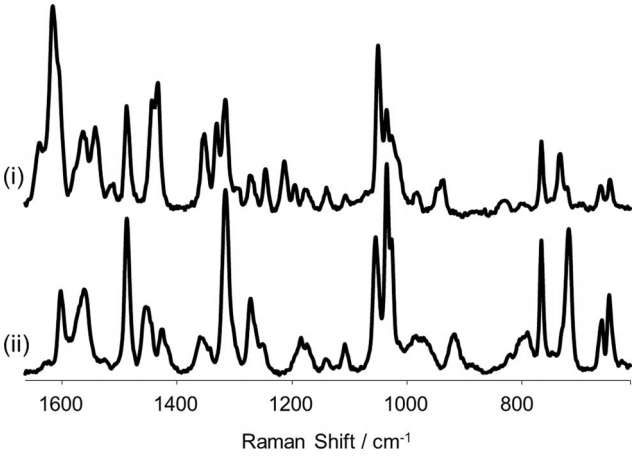

Figure 13. SERS spectra of (i) $[Ru(bpy)_2(pyrphen)]^{2+}$ and (ii) $[Ru(bpy)_2(thimphen)]^{2+}$ obtained by aggregation of gold colloid (λ_{exc} = 785 nm).

surface, but it remains unclear what specific structural changes occur. Previously, Shimoyama and coworkers observed a change in intensity of an absorption at 720 cm^{-1} in the FTIR spectrum of a monolayer of thiophene, over time, which they assigned to a rearrangement in the packing of the thiophene on the gold substrate.[29,30] It was proposed, albeit on the basis of a relatively small data set, that thiophene initially lays flat on the surface and over time rearranges to a tightly packed upstanding monolayer. Considering the geometry and measured surface densities of the complexes $[Ru(bpy)_2(thimphen)]^{2+}$ and $[Ru(bpy)_2(pyrphen)]^{2+}$, neither of these two modes of packing seems reasonable for these complexes and hence an alternative interpretation of a chemical reaction involving the thiophenes is more appropriate in the present case.

An equimolar mixture of $[Ru(D_8\text{-}bpy)_2(thimphen)]^{2+}$ and $[Ru(bpy)_3]^{2+}$ was used for SAM formation to investigate the relative importance of chemisorption and physisorption. A SERS spectrum of the same solution was obtained by aggregation of gold colloid; in this case the intensity ratio was different from the spectra obtained for SAMs on roughened gold beads (Figure 14).

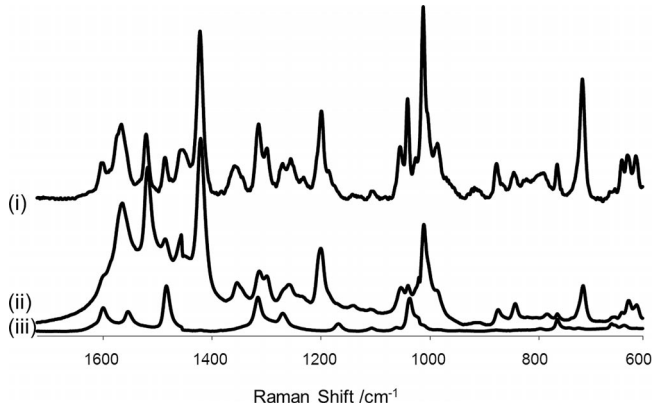

Figure 14. (i) A SERS spectrum obtained by aggregation of gold colloid using a 1:1 mixture of $[Ru(D_8\text{-}bpy)_2(thimphen)]^{2+}$ and $[Ru(bpy)_3]^{2+}$ in ethanol, (ii) a SERS spectrum obtained on a roughened gold bead with a SAM formed from the same solution and (iii) a SERS spectrum obtained on a roughened gold bead with a SAM formed from an ethanol solution of $[Ru(bpy)_3]^{2+}$ only (λ_{exc} = 785 nm). Surfaces were rinsed with ethanol after SAM formation before spectra were recorded.

The Raman spectrum obtained from the SAM formed from an equimolar mixture of $[Ru(bpy)_3]^{2+}$ and $[Ru(D_8\text{-}bpy)_2(thimphen)]^{2+}$ in ethanol indicates that $[Ru(D_8\text{-}bpy)_2(thimphen)]^{2+}$ binds to the roughened gold electrode more than $[Ru(bpy)_3]^{2+}$ does. The intensity of the bands from $[Ru(D_8\text{-}bpy)_2(thimphen)]^{2+}$ in the SERS spectrum obtained from the gold bead are relatively more intense than the bands from $[Ru(bpy)_3]^{2+}$ in comparison to spectra obtained upon aggregation of gold colloid (Figure 14). This indicates that the differences in intensity of the two complexes in the monolayer on a gold bead are not due to differences in surface enhancement, but due to a different surface density of both complexes. These data demonstrate that although physisorption is important in the formation of monolayers, the thiophene unit is actively involved in surface anchoring.

Conclusions

Four novel mononuclear transition metal complexes have been synthesised with ruthenium or osmium at the metal centre. Electrochemical characterisation using cyclic voltammetry reveals one metal-based oxidation as well as several ligand-based reductions for each complex. The data obtained show that for all four complexes monolayers can be formed, on both Pt and Au. Importantly the thiophene-based compounds show monolayer formation and SERS spectroscopy indicates that the thiophene ring is actively involved in binding to gold. Considerable attention has been paid in the literature to the investigation of thiol-type

linkers containing –SH, or precursor –SR groups.[10] These linkers bind well to surfaces, however, the introduction of such tethers often presents synthetic challenges with regard to the synthesis of redox active units especially when they are introduced in osmium compounds. The reason for this is their limited thermal stability and that they often decompose under the high temperatures required during synthesis of osmium complexes. On the other hand the synthetic procedures for the thiophene analogues are straightforward. The introduction of thiophene moieties therefore opens a promising novel approach to the immobilisation of redox active species with sulfur-based linkers on Au and Pt surfaces. However, a key question arises as to the nature of the interaction in systems employing these anchors with regard to the relative contribution of physisorption and chemisorption. Indeed as we have shown, even without the anchor unit significant physisorption takes place for complexes such as $[Ru(bpy)_3]^{2+}$ and hence the addition of an imidazole-pyridine/thiophene unit may contribute towards immobilisation on surfaces through physisorption to a significant extent.

Experimental Section

Materials: The compounds 1,10-phenanthroline-5,6-dione,[13] 2-(3-thio)imidazo[*f*]-1,10-phenanthroline (thimphen),[13,31] D_8-2,2′-bipyridyl,[32] $[Ru(bpy)_2Cl_2]\cdot 2H_2O$,[33] $[Os(bpy)_2Cl_2]\cdot 2H_2O$,[34] $[Ru(D_8\text{-}bpy)_2Cl_2]\cdot 2H_2O$, $[Os(D_8\text{-}bpy)_2Cl_2]\cdot 2H_2O$, $[Ru(bpy)_2(phen)](PF_6)_2$,[35] $[Os(bpy)_2(phen)](PF_6)_2$ and $[Ru(bpy)_2(phendione)](PF_6)_2$[36] were synthesised according to literature procedures. All other chemicals were purchased from commercial sources and used without further purification unless stated otherwise. All solvents used for synthesis were of reagent grade. All solvents used for spectroscopic measurements were of HPLC grade or better. The synthesis and ^1H NMR characterisation of the complexes $[Ru(bpy)_2(thimphen)](PF_6)_2$, $[Os(bpy)_2(thimphen)](PF_6)_2$, $[Ru(D_8\text{-}bpy)_2(thimphen)](PF_6)_2$, $[Ru(bpy)_2(pyrphen)](PF_6)_2$, $[Ru(D_8\text{-}bpy)_2(pyrphen)](PF_6)_2$, $[Os(bpy)_2(phendione)](PF_6)_2$ and $[Os(bpy)_2(pyrphen)](PF_6)_2$ are provided as Supporting Information.

Instrumental Methods: ^1H NMR spectra were recorded with a Bruker Avance 400 MHz NMR spectrometer. Data are relative to residual solvent signals. UV/Vis absorption spectra were recorded with a JASCO 570 UV/Vis/NIR spectrophotometer using 1 cm pathlength quartz cells. Electrochemical experiments were carried out using a CH Instruments Version 8.15 software controlled electrochemical bipotentiostat (CHI750C or CHI760C). Glassy carbon (3-mm-diameter disk), platinum (2-mm-diameter disk) and gold bead electrodes were cleaned by standard methods. A Pt wire was used as the counter electrode. A saturated calomel electrode (SCE), $Hg/HgSO_4$ or Ag/AgCl wire, were used as reference electrodes. The electrochemical potentials are reported with respect to SCE. Tetrabutylammonium perchlorate ($TBAClO_4$, Fluka, electrochemical grade ≥99.0%) in acetonitrile (Aldrich anhydrous, 99.8%) or dichloromethane (Aldrich, anhydrous, 99.8%) were used as electrolyte and solvent, respectively. For the preparation of electrodes for the self-assembled monolayer formation the solvent was purged with argon for at least 10 min prior to experiments and a blanket of argon was maintained throughout.

Resonance Raman spectra were obtained at λ_{exc} = 449 nm (35 mW, PowerTechnology), 473 (100 mW, Cobolt Lasers) and 355 nm (10 mW, Cobolt Lasers). A 5-cm-diameter plano-convex lens (f = 6 cm) was used and Raman scattering was collected in a 180° backscattering arrangement. The collimated Raman scattering was focused by a second 5-cm-diameter plano-convex lens (f = 6 cm) through an appropriate long-pass edge filter (Semrock) into a Shamrock300 spectrograph (Andor Technology) with a 1200 lmm^{-1} grating blazed at 500 nm and collected by a Newton EMCCD (Andor Technology) operating in conventional CCD mode. Data were recorded and processed using the program Solis (Andor Technology). The spectral calibration was performed using the Raman spectrum of acetonitrile/toluene, 50:50 (v:v). Emission spectra were recorded using the same system as for Raman spectroscopy except that a 150 lmm^{-1} grating was employed. Samples were held in quartz 10-mm-pathlength cuvettes. Surface-enhanced Raman scattering (SERS) spectra were recorded using a Perkin–Elmer Raman station with excitation at 785 nm. For solution SERS spectra, complexes were dissolved in water prior to addition to the Au colloid, which induced aggregation of the colloid directly. SERS spectra of monolayers were obtained on gold bead electrodes prepared using an adaptation of the procedure[37] originally described by Tian et al.[38] See Supporting Information for details.

Computational Details: Molecular structures were optimised within the framework of density functional theory (DFT) employing the BP86 functional[39,40,41] with a split-valence SV(P) basis set[42] in combination with conductor-like screening (dielectric constant $\varepsilon = \infty$ through the solvation model COSMO[43]). These calculations were performed with the program package Turbomole[44] using the efficient RI-J approximation.[45] Population analyses were performed with the Gaussian 09[46] program at the BP86/def-TZVP level of theory in an electric conductor environment (IEF-PCM formalism, acetonitrile) using the previously optimized molecular geometries. Percentage contributions were evaluated using GaussSum.[47]

Supporting Information (see footnote on the first page of this article): Details of synthesis and characterisation of all complexes, ^1H NMR spectra and additional UV/Vis absorption and Raman data and procedures for preparation of SAMs. Additional DFT data tables are provided.

Acknowledgments

The Netherlands Organisation for Science (NWO) (VIDI grant 700.57.428, to H. L. and W. R. B.), the University of Groningen (Ubbo Emmius scholarship to A. D.) and the Science Foundation Ireland (grant number 06/RFP/029CL, to Y. H. and J. G. V.) are acknowledged for financial support.

[1] P. J. Low, *Dalton Trans.* **2005**, 2821–2824.
[2] J. M. Tour, *Acc. Chem. Res.* **2000**, *33*, 791–804.
[3] a) V. Balzani, A. Credi, M. Venturi, *Molecular Devices and Machines - A Journey into the Nano World*, Wiley-VCH, Weinheim, Germany, **2003**; b) M. Lundstrom, *Science* **2003**, *299*, 210–211; c) P. A. Packan, *Science* **1999**, *285*, 2079–2081.
[4] R. L. McCreery, A. J. Bergren, *Adv. Mater.* **2009**, *21*, 4303–4322.
[5] a) L. A. Bumm, J. J. Arnold, M. T. Cygan, T. D. Dunbar, T. P. Burgin, L. Jones, D. L. Allara, J. M. Tour, P. S. Weiss, *Science* **1996**, *271*, 1705–1707; b) S. J. Tans, M. H. Devoret, H. J. Dai, A. Thess, R. E. Smalley, L. J. Geerligs, C. Dekker, *Nature* **1997**, *386*, 474–477.
[6] a) N. B. Zhitenev, H. Meng, Z. Bao, *Phys. Rev. Lett.* **2002**, *88*, 226801-1; b) S. Kubatkin, A. Danilov, M. Hjort, J. Cornil, J. L. Bredas, N. Stuhr-Hansen, P. Hedegard, T. Bjornholm, *Nature*

2003, *425*, 698–701; c) J. Park, A. N. Pasupathy, J. I. Goldsmith, C. Chang, Y. Yaish, J. R. Petta, M. Rinkoshi, J. P. Sethna, H. D. Abruna, P. L. McEuen, D. C. Ralph, *Nature* **2002**, *417*, 722–723.
[7] a) M. A. Reed, *Proc. IEEE* **1999**, *87*, 652–658; b) R. M. Metzger, *Chem. Rev.* **2003**, *103*, 3803–3834; c) M. K. Ng, D. C. Lee, L. Yu, *J. Am. Chem. Soc.* **2002**, *124*, 11862–11863.
[8] a) R. J. Forster, L. R. Faulkner, *J. Am. Chem. Soc.* **1994**, *116*, 5444–5452; b) R. J. Forster, L. R. Faulkner, *J. Am. Chem. Soc.* **1994**, *116*, 5453–5461.
[9] a) T. Albrecht, A. Guckian, J. Ulstrup, J. G. Vos, *IEEE Trans. On Nanotechnology* **2005**, *4*, 430–434; b) T. Albrecht, A. Guckian, J. Ulstrup, J. G. Vos, *Nano Lett.* **2005**, *5*, 1451–1455; c) T. Albrecht, K. Moth-Poulsen, J. B. Christensen, A. Guckian, T. Bjornholm, J. G. Vos, J. Ulstrup, *J. Chem. Soc., Faraday Trans.* **2006**, *131*, 265–279; d) T. Albrecht, A. Guckian, A. M. Kuznetsov, J. G. Vos, J. Ulstrup, *J. Am. Chem. Soc.* **2006**, *128*, 17132–17138.
[10] J. S. Lindsey, D. F. Bocian, *Acc. Chem. Res.* **2011**, *44*, 638–650 and references cited therein.
[11] N. M. O'Boyle, T. Albrecht, D. H. Murgida, L. Cassidy, J. Ulstrup, J. G. Vos, *Inorg. Chem.* **2007**, *46*, 117–124.
[12] E. O. Sako, H. Kondoh, I. Nakai, A. Nambu, T. Nakamura, T. Ohta, *Chem. Phys. Lett.* **2005**, *413*, 267–271.
[13] T. Cardinaels, J. Ramaekers, D. Guillon, B. Donnio, K. Binnemans, *J. Am. Chem. Soc.* **2005**, *127*, 17602–17603.
[14] a) K. A. Goldsby, T. J. Meyer, *Inorg. Chem.* **1984**, *23*, 3002–3010; b) E. M. Kober, Thesis, North Carolina, US, **1982**; c) E. M. Kober, T. J. Meyer, *Inorg. Chem.* **1984**, *23*, 3877–3886; d) E. M. Kober, T. J. Meyer, *Inorg. Chem.* **1982**, *21*, 3967–3977.
[15] a) J. C. Curtis, J. S. Bernstein, T. J. Meyer, *Inorg. Chem.* **1985**, *24*, 385–397; b) K. S. Schanze, T. J. Meyer, *Inorg. Chem.* **1985**, *24*, 2121–2123.
[16] E. M. Kober, J. V. Caspar, R. S. Lumpkin, T. J. Meyer, *J. Phys. Chem.* **1986**, *90*, 3722–3734.
[17] a) C. Long, J. G. Vos, *Inorg. Chim. Acta* **1984**, *89*, 123–131; b) B. E. Buchanan, J. G. Vos, M. Kaneko, W. J. M. van der Putten, J. M. Kelly, R. Hage, R. Prins, J. G. Haasnoot, J. Reedijk, R. A. G. de Graaff, *J. Chem. Soc., Dalton Trans.* **1990**, 2425–2431.
[18] J. G. Vos, *Polyhedron* **1992**, *11*, 2285–2299.
[19] W. R. Browne, N. M. O'Boyle, J. J. McGarvey, J. G. Vos, *Chem. Soc. Rev.* **2005**, *34*, 641–663.
[20] J. Z. Wu, B. H. Ye, L. Wang, L. N. Ji, J. Y. Zhou, R. H. Li, Z. Y. Zhou, *J. Chem. Soc., Dalton Trans.* **1997**, 1395–1401.
[21] M. M. Cooke, E. H. Doeven, C. F. Hogan, J. L. Adcock, G. P. McDermott, X. A. Conlon, N. W. Barnett, F. M. Pfeffer, P. S. Francis, *Anal. Chim. Acta* **2009**, *635*, 94–101.
[22] R. Hage, *Ph. D. Thesis*, Leiden University, The Netherlands, **1991**.
[23] The cathodic wave at –2.38 V is present in the CV of the electrolyte only.
[24] R. J. Forster, T. E. Keyes, J. G. Vos, *Interfacial Supramolecular Assemblies*, John Wiley & Sons, Chichester, England, **2003**.
[25] P. Bertoncello, E. T. Kefalas, Z. Pikramenou, P. R. Unwin, R. J. Forster, *J. Phys. Chem. B* **2006**, *110*, 10063–10069.
[26] R. J. Forster, Y. Pellegrin, D. Leane, J. L. Brennan, T. E. Keyes, *J. Phys. Chem. C* **2007**, *111*, 2063–2068.
[27] R. L. Aggarwal, L. W. Farrar, N. G. Greeneltch, R. P. Van Duyne, D. L. Polla, *Appl. Spectrosc.* **2012**, *66*, 740–743.
[28] P. K. Mallick, G. D. Danzer, D. P. Strommen, J. R. Kincaid, *J. Phys. Chem.* **1988**, *92*, 5628–5632.
[29] T. Matsuura, M. Nakajima, Y. Shimoyama, *Jpn. J. Appl. Phys.* **2001**, *40*, 6945–6950.
[30] T. Matsuura, Y. Shimoyama, *Eur. Phys. J. E* **2002**, *7*, 233–240.
[31] J.-Z. Wu, L. Li, T.-X. Zeng, L.-J. Ji, J.-Y. Zhou, T. Luo, R.-H. Li, *Polyhedron* **1997**, *16*, 103–107.
[32] W. R. Browne, C. M. O'Connor, J. S. Killeen, A. L. Guckian, M. Burke, P. James, M. Burke, J. G. Vos, *Inorg. Chem.* **2002**, *41*, 4245–4251.
[33] B. P. Sullivan, D. J. Salmon, T. J. Meyer, *Inorg. Chem.* **1978**, *17*, 3334–3341.
[34] D. A. Buckingham, F. P. Dwyer, H. A. Goodwin, A. M. Sargeson, *Aust. J. Chem.* **1964**, *17*, 325–336.
[35] W. Huang, T. Ogawa, *Polyhedron* **2006**, *25*, 1379–1385.
[36] S. D. Bergman, M. Koi, *Inorg. Chem.* **2005**, *44*, 1647–1656.
[37] M. E. Abdelsalam, P. N. Bartlett, J. J. Baumberg, S. Cintra, T. A. Kelf, A. E. Russell, *Electrochem. Commun.* **2005**, *7*, 740–744.
[38] Z. Q. Tian, B. Ren, D. Y. Wu, *J. Phys. Chem. B* **2002**, *106*, 9463–9483.
[39] A. D. Becke, *Phys. Rev. A* **1988**, *38*, 3098–3100.
[40] J. P. Perdew, *Phys. Rev. B* **1986**, *33*, 8822–8824; Erratum: *Phys. Rev. B* **1986**, *34*, 7406.
[41] S. H. Vosko, L. Wilk, M. Nusair, *Can. J. Phys.* **1980**, *58*, 1200–1211.
[42] A. Schäfer, H. Horn, R. Ahlrichs, *J. Chem. Phys.* **1992**, *97*, 2571–2577.
[43] A. Klamt, G. Schüürmann, *J. Chem. Soc. Perkin Trans. 2* **1993**, 799–805.
[44] R. Ahlrichs, M. Bär, M. Häser, H. Horn, C. Kölmel, *Chem. Phys. Lett.* **1989**, *162*, 165–169.
[45] K. Eichkorn, O. Treutler, H. Ohm, M. Häser, R. Ahlrichs, *Chem. Phys. Lett.* **1995**, *240*, 283–289; Erratum: *Chem. Phys. Lett.* **1995**, *242*, 652–660.
[46] M. J. Frisch, G. W. Trucks, H. B. Schlegel, G. E. Scuseria, M. A. Robb, J. R. Cheeseman, G. Scalmani, V. Barone, B. Mennucci, G. A. Petersson, H. Nakatsuji, M. Caricato, X. Li, H. P. Hratchian, A. F. Izmaylov, J. Bloino, G. Zheng, J. L. Sonnenberg, M. Hada, M. Ehara, K. Toyota, R. Fukuda, J. Hasegawa, M. Ishida, T. Nakajima, Y. Honda, O. Kitao, H. Nakai, T. Vreven, J. J. A. Montgomery, J. E. Peralta, F. Ogliaro, M. Bearpark, J. J. Heyd, E. Brothers, K. N. Kudin, V. N. Staroverov, R. Kobayashi, J. Normand, K. Raghavachari, A. Rendell, J. C. Burant, S. S. Iyengar, J. Tomasi, M. Cossi, N. Rega, J. M. Millam, M. Klene, J. E. Knox, J. B. Cross, V. Bakken, C. Adamo, J. Jaramillo, R. Gomperts, R. E. Stratmann, O. Yazyev, A. J. Austin, R. Cammi, C. Pomelli, J. W. Ochterski, R. L. Martin, K. Morokuma, V. G. Zakrzewski, G. A. Voth, P. Salvador, J. J. Dannenberg, S. Dapprich, A. D. Daniels, O. Farkas, J. B. Foresman, J. V. Ortiz, J. Cioslowski, D. J. Fox, *Gaussian 09*, rev. A.02, **2009**, Wallingford, CT.
[47] N. M. O'Boyle, A. L. Tenderholt, K. M. Langner, *J. Comput. Chem.* **2008**, *29*, 839–845.

Received: March 17, 2013
Published Online: June 17, 2013

